Journal of Computational Physics 229 (2010) 7747–7764

Contents lists available at ScienceDirect

Journal of Computational Physics

journal homepage: www.elsevier.com/locate/jcp

A unified gas-kinetic scheme for continuum and rarefied flows

Kun Xu [a,*], Juan-Chen Huang [b]

[a] Mathematics Department, Hong Kong University of Science and Technology, Clear Water Bay, Kowloon, Hong Kong
[b] Department of Merchant Marine, National Taiwan Ocean University, Keelung 20224, Taiwan

ARTICLE INFO

Article history:
Received 12 February 2010
Received in revised form 5 May 2010
Accepted 16 June 2010
Available online 25 June 2010

Keywords:
Unified scheme
Navier–Stokes equations
Free molecule flow

ABSTRACT

With discretized particle velocity space, a multiscale unified gas-kinetic scheme for entire Knudsen number flows is constructed based on the BGK model. The current scheme couples closely the update of macroscopic conservative variables with the update of microscopic gas distribution function within a time step. In comparison with many existing kinetic schemes for the Boltzmann equation, the current method has no difficulty to get accurate Navier–Stokes (NS) solutions in the continuum flow regime with a time step being much larger than the particle collision time. At the same time, the rarefied flow solution, even in the free molecule limit, can be captured accurately. The unified scheme is an extension of the gas-kinetic BGK-NS scheme from the continuum flow to the rarefied regime with the discretization of particle velocity space. The success of the method is due to the un-splitting treatment of the particle transport and collision in the evaluation of local solution of the gas distribution function. For these methods which use operator splitting technique to solve the transport and collision separately, it is usually required that the time step is less than the particle collision time. This constraint basically makes these methods useless in the continuum flow regime, especially in the high Reynolds number flow simulations. Theoretically, once the physical process of particle transport and collision is modeled statistically by the kinetic Boltzmann equation, the transport and collision become continuous operators in space and time, and their numerical discretization should be done consistently. Due to its multiscale nature of the unified scheme, in the update of macroscopic flow variables, the corresponding heat flux can be modified according to any realistic Prandtl number. Subsequently, this modification effects the equilibrium state in the next time level and the update of microscopic distribution function. Therefore, instead of modifying the collision term of the BGK model, such as ES-BGK and BGK–Shakhov, the unified scheme can achieve the same goal on the numerical level directly. Many numerical tests will be used to validate the unified method.

1. Introduction

The development of accurate numerical methods for all flow regimes is challenging. An excellent example is the nozzle flow for controlling aerospace orbit, where both continuum and vacuum flows exist from gas container to the nozzle exit. Both the kinetic methods, such as direct simulation Monte Carlo (DSMC), and modern CFD techniques based on the Navier–Stokes (NS) equations, encounter computational difficulties when applied to these flows. The DSMC method requires that the time step and cell size are less than the particle collision time and mean free path, which subsequently introduce enormous computational cost in the high density regime. On the other hand, the conventional continuum NS methods are

* Corresponding author. Tel.: +852 2358 7433; fax: +852 2358 1643.
E-mail addresses: makxu@ust.hk (K. Xu), jchuang@mail.ntou.edu.tw (J.-C. Huang).

0021-9991/$ - see front matter © 2010 Elsevier Inc. All rights reserved.
doi:10.1016/j.jcp.2010.06.032

inapplicable for capturing non-equilibrium effects in the rarefied flow regime. High-order hydrodynamic equations are mostly limited to the transition flow regime only [22]. In recent years, the hybrid methods which combine NS and kinetic approaches have been often used to model flows which have both continuum and rarefied regimes [26,27,9,5,30,8,32]. A buffer zone is used to couple different approaches with the assumption of correctness of both methods in this zone. These approaches may sensitively depend on the location of the interface between different methods. Certainly, it is required that both methods are reliable in the buffer zone. But, in reality it may become that neither method can be applied there. For example, in many hybrid methods, it is assumed that in the buffer zone the flow can be correctly described by the NS equations, which means that the extension of the kinetic approach to the buffer zone should have the correct NS limit as well. But, this is just the difficult part for the kinetic approach. So, in order to accurately simulate the whole flow regimes, it is still desirable to have a single kinetic method which presents accurately the NS solution in the continuum flows and the collisionless Boltzmann solution in the free molecule regime. This can be done dynamically through the numerical discretization of the Boltzmann equation, instead of geometrically through the zone separations.

The Boltzmann equation describes the time evolution of the density distribution of a monatomic dilute gas with binary elastic collisions. The fluid dynamic Navier–Stokes (NS), Burnett and Super-Burnett equations can be derived from the Boltzmann equation. The Boltzmann equation is valid from the continuum flow regime to the free molecule flow. So, theoretically a unified kinetic method which is valid in the whole range of Knudsen number can be developed once the numerical discretization is properly designed. In the framework of deterministic approximation, the most popular class of methods is based on the so-called discrete velocity methods (DVM) or discrete ordinate method (DOM) of the Boltzmann equation [7,38,16,18,1,13]. These methods use regular discretization of particle velocity space. Most of these methods can give accurate numerical solution for high Knudsen number flows, such as those from the upper transition to the free molecule regime. However, in the continuum flow regime, it is recognized that they have difficulty in the capturing of the Navier–Stokes solutions, especially for the high Reynolds number flows, where the intensive particle collisions take place. Under this situation, the requirement of the time step being less than the particle collision time makes these methods prohibitive in the continuum flow application. In order to get unconditionally stable schemes with large time step, it is natural to use implicit or semi-implicit method for the collision part [18,24,11]. However, even though a scheme could overcome the stability restriction and use large time step, there is still accuracy concern. Because these schemes have the same numerical mechanism as the flux vector splitting (FVS) methods, their intrinsic numerical dissipation is proportional to time step [35], which deteriorates the NS solution when a large time step is used.

In order to develop a kinetic scheme for the whole flow regime, much effort has been paid on the development of the so-called asymptotic preserving (AP) scheme. As defined in [11], a kinetic scheme is AP if (1) it preserves the discrete analogy of the Chapman–Enskog expansion when the Knudsen numbers go to 0. (2) in the continuum regime, the time step is not restricted by the particle collision time. Besides the above two conditions, we may need a third one as well, (3) the scheme has at least second-order accuracy in both continuum and free molecule regimes. Therefore, the AP scheme is the appropriate choice to solve the kinetic equation. For example, for an AP scheme in the nozzle simulation, with a uniform time step in the whole domain, this time step must be much larger than the particle collision time in the inner high density region, and be the same order or less in the outer rarefied and free molecular regions. Many kinetic approaches have been developed to target on the kinetic AP methods [2,9,11,24]. One of the above AP schemes for the NS asymptotic in the continuum regime is the method developed by Bennoune et al. [2]. Their deterministic method is based on a decomposition of the Boltzmann equation into a system which couples a kinetic equation (non-equilibrium) with a fluid one (equilibrium). The fluid part of this system degenerates, for small particle collision time, into the NS equations. However, in the collisionless limit, the physical basis and numerical formulation of separating a distribution function into an equilibrium and a non-equilibrium part is questionable. The accuracy of the above scheme in the collisionless limit has to be tested as well. In other words, AP scheme should not only have the accuracy in the continuum flow regime, the validity of the kinetic method in the collisionless limit should be kept as well.

In order to develop an AP scheme for the kinetic equation, we need a correct understanding of the Boltzmann equation. Even though the individual particle movement has distinct transport and collision process, once this process is described by a statistical model, such as the Boltzmann equation, the transport and collision processes are coupled everywhere in space and time. To separate them numerically, such as the operator splitting methods, is inconsistent with the underlying physical model. As shown in this paper, a simple upwinding discretization for the particle transport term in the Boltzmann equation, i.e., uf_x term, is basically an operator splitting approach and introduces difficulties to get AP property. Without correctly discretizing this term, any other modification in the kinetic method may not work properly in the whole flow regime. In the high Knudsen number flow regime, the decoupling of transport and collision may not become a problem, because the numerical error introduced due to the decoupling (being proportional to time step) is much less than the physical one (being proportional to particle collision time). But, it cannot be tolerated in the continuum flow regime, especially for an AP method.

In the past years, the gas-kinetic BGK–NS scheme for the Navier–Stokes solutions has been well developed [34], and has been successfully applied for the continuum flow simulations from nearly incompressible to hypersonic viscous and heat conducting flows [29,36,37,17,15]. In the BGK–NS method, the particle velocity space is continuous and is integrated out in the flux evaluations in a finite volume scheme. This is not surprised because in the fluid regime, based on the Chapman–Enskog expansion the gas distribution function for the viscous flow is well-defined. Therefore, the efficiency of the BGK–NS method is similar to the traditional NS flow solver, where the same CFL condition is used for the determination of time step. Theoretically, any kinetic scheme with NS asymptotic AP property should be able to recover the BGK–NS

scheme in the continuum limit. So, in this paper we are going to extend the BGK–NS method from the continuum flow to the rarefied regime, which includes the free molecule limit. In order to do that, we have to discretize the particle velocity space as well, because the real gas distribution function in the highly non-equilibrium region can be hardly described by a Maxwellian distribution function and its derivatives. So, the current method can be also considered as a discrete velocity version of the BGK-NS scheme.

This paper is organized in the following. Section 2 is about the introduction of kinetic BGK model and the discrete ordinate method (DOM). Section 3 presents the current unified multiscale method for the whole Knudsen number flow simulations. Section 4 is the analysis of the unified scheme, especially about the modification of Prandtl number of the unified scheme. Section 5 includes many numerical tests to validate the current method. The last section is the conclusion.

2. Kinetic theory and discrete ordinate method

In this paper, we will present a unified scheme for all Knudsen number flows. The one-dimensional kinetic equation will be used to illustrate the idea. In this section, we are going to first introduce the kinetic equation and the traditional discrete ordinate method (DOM).

The one-dimensional gas-kinetic BGK equation can be written as [6,3]

$$f_t + uf_x = \frac{g-f}{\tau}, \tag{1}$$

where f is the gas distribution function and g is the equilibrium state approached by f. Both f and g are functions of space x, time t, particle velocities u, and internal variable ξ. The particle collision time τ is related to the viscosity and heat conduction coefficients, i.e., $\tau = \mu/p$ where μ is the dynamic viscosity coefficient and p is the pressure. The equilibrium state is a Maxwellian distribution,

$$g = \rho\left(\frac{\lambda}{\pi}\right)^{\frac{K+1}{2}} e^{-\lambda((u-U)^2+\xi^2)},$$

where ρ is the density, U is the macroscopic velocity in the x direction, λ is equal to $m/2kT$, m is the molecular mass, k is the Boltzmann constant, and T is the temperature. For 1D flow, the total number of degrees of freedom K in ξ is equal to $(3-\gamma)/(\gamma-1)$. For example, for a monatomic gas with $\gamma = 5/3$, K is equal to 2 to account for the particle motion in the y and z-directions. In the equilibrium state, the internal variable ξ^2 is equal to $\xi^2 = \xi_1^2 + \xi_2^2 + \cdots + \xi_K^2$. The relation between mass ρ, momentum ρU, and energy E densities with the distribution function f is

$$\begin{pmatrix} \rho \\ \rho U \\ E \end{pmatrix} = \int \psi_\alpha f d\Xi, \quad \alpha = 1,2,3, \tag{2}$$

where ψ_α is the component of the vector of moments

$$\boldsymbol{\psi} = (\psi_1, \psi_2, \psi_3)^T = \left(1, u, \frac{1}{2}(u^2+\xi^2)\right)^T,$$

and $d\Xi = du\, d\xi_1 d\xi_2 \ldots d\xi_K$ is the volume element in the phase space with $d\xi = d\xi_1 d\xi_2 \ldots d\xi_K$. Based on the distribution function f, all other macroscopic flow variables, such as the stress p_{ij} and heat fluxes q_i, can be defined as well,

$$p_{ij} = \int (u_i - U_i)(u_j - U_j) f d\Xi,$$
$$q_i = \int \frac{1}{2}(u_i - U_i)((u_j - U_j)^2 + \xi^2) d\Xi,$$

where U_i is the averaged fluid velocity $U_i = \int u_i f d\Xi / \int f d\Xi$. Since mass, momentum, and energy are conserved during particle collisions, f and g satisfy the conservation constraint,

$$\int (g-f)\psi_\alpha d\Xi = 0, \quad \alpha = 1,2,3, \tag{3}$$

at any point in space and time.

Before we introduce discrete ordinate method, let's first discretize the physical space, time, and particle velocity space. The physical space is divided into numerical cells with cell size Δx, and the jth-cell is given by $x \in [x_{j-1/2}, x_{j+1/2}]$ with cell size $\Delta x = x_{j+1/2} - x_{j-1/2}$. The temporal discretization is denoted by t^n for the nth-time step. The particle velocity space is discretized by $2N+1$ subcells with cell size Δu, and the center of kth-velocity interval is $u_k = k\Delta u$, and it represents the average velocity u in that interval,

$$u \in \left[\left(k-\frac{1}{2}\right)\Delta u, \left(k+\frac{1}{2}\right)\Delta u\right], \quad k = -N, -(N-1), \ldots, -1, 0, 1, \ldots, (N-1), N.$$

Then, the averaged gas distribution function in cell j, at time step t^n, and around particle velocity u_k, is given by

$$f(x_j,t^n,u_k)=f_{j,k}^n=\frac{1}{\Delta x\Delta u}\int_{x_{j-1/2}}^{x_{j+1/2}}\int_{u_k-\frac{1}{2}\Delta u}^{u_k+\frac{1}{2}\Delta u}f(x,t^n,u)dxdu, \tag{4}$$

where Δx is the cell size and Δu is the particle velocity interval defined later.

The BGK Eq. (1) can be written as

$$f_t=-uf_x+\frac{g-f}{\tau}. \tag{5}$$

Integrating the above equation in a control volume $\int_{x_{j-1/2}}^{x_{j+1/2}}\int_{t^n}^{t^{n+1}}(\ldots)dxdt/\Delta x$, and keeping the particle velocity space continuous, the above differential equation becomes an integral equation

$$f_j^{n+1}=f_j^n+\frac{1}{\Delta x}\int_{t^n}^{t^{n+1}}\left(u\hat{f}_{j-1/2}(t)-u\hat{f}_{j+1/2}(t)\right)dt+\frac{1}{\Delta x}\int_{t^n}^{t^{n+1}}\int_{x_{j-1/2}}^{x_{j+1/2}}\frac{g-f}{\tau}dxdt, \tag{6}$$

where $\hat{f}_{j+1/2}$ is the gas distribution function at the cell interface $x_{j+1/2}$. The above equation is exact and there is no any numerical error introduced yet. For a kinetic scheme, two terms on the right hand side of the above equation have to be numerically evaluated.

With discretized particle velocity space, at each particle velocity u_k a standard operator splitting method is to solve the above equation in the following steps [8,38]. Eq. (6) is decoupled to

$$f_{j,k}^*=f_{j,k}^n+\frac{1}{\Delta x}\int\left(u_k\hat{f}_{j-1/2,k}(t)-u_k\hat{f}_{j+1/2,k}(t)\right)dt, \tag{7}$$

for the transport across a cell interface, and

$$\frac{df_{j,k}}{dt}=\frac{g-f_{j,k}^*}{\tau}, \tag{8}$$

for the particle collision or source term inside each cell. In the transport part, the collisionless Boltzmann equation or upwinding approach, is used,

$$f_t+uf_x=0, \tag{9}$$

for the flux evaluation at the cell interface. For example, for a 1st-order method, the upwinding flux is based on the following solution at the cell interface,

$$\hat{f}_{j+1/2,k}=\begin{cases}f_{j,k}, & u_k\geqslant 0,\\ f_{j+1,k}, & u_k<0,\end{cases} \tag{10}$$

which is dynamically equivalent to the flux vector splitting scheme. The above transport and collision steps can be also coupled using Runge–Kutta method within a time step.

If we take conservative moments ψ_α on Eq. (6), due to the conservation of conservative variables during particle collision process, the update of conservative variables become

$$W_j^{n+1}=W_j^n+\frac{1}{\Delta x}\int_{t^n}^{t^{n+1}}\left(F_{j-1/2}(t)-F_{j+1/2}(t)\right)dt, \tag{11}$$

where W is the averaged conservative mass, momentum, and energy densities inside each cell, and $F=\int u\psi_\alpha\hat{f}d\Xi$ is the flux based on the collisionless Boltzmann equation. The above scheme for the update of macroscopic flow variables is physically identical to the kinetic flux vector splitting schemes (KFVS) [25,10]. The only difference is the approximation of initial gas distribution function used at the beginning of each time step in order to evaluate the interface flux $\hat{f}$. For the KFVS scheme, an equilibrium state with continuous particle velocity space is used to construct initial condition f for Eq. (9), and for the DOM the initial f is explicitly given from the update of the discretized particle distribution function. But, the different initial condition will not change the numerical dissipative mechanism in the KFVS method, where the numerical dissipation is proportional to the time step. Therefore, if a large time step could be used for the DOM method in the continuum flow regime, the numerical dissipation would make DOM scheme be inaccurate for the NS solutions. It is a well-known defect for all flux vector splitting methods [31,35]. So, in the continuum flow regime, for the DOM method the requirement of time step being less than the particle collision time helps the scheme not only for the stability, but also for the accuracy. Unfortunately, this constraint deviates the above scheme away from an AP method for the NS solutions in the continuum flow regime.

In order to design an AP scheme which is able to capture NS solutions in the continuum flow regime and also get an accurate free molecule solution in another limit, the full BGK Eq. (1) has to be solved in the flux evaluation in Eq. (6) across a cell interface. The kinetic equation models the transport $uf_x(x,t)$ and collision $(g-f)/\tau$ as a continuous function of x and t. For these molecules passing through a cell interface, they do suffer from particle collisions during their passage moving towards

to the cell interface. The collision frequency of these molecules distinguishes the continuum and rarefied flow regimes dynamically, subsequently presents the corresponding distribution functions.

3. Unified kinetic scheme for all flow regimes

In this section, we will present a unified kinetic scheme based on the BGK model for all flow regimes. The current method is a natural extension of the gas-kinetic BGK-NS method for the compressible Navier–Stokes solutions to all Knudsen number flows. In this section, only one-dimensional formulation will be presented. The extension to 2D and 3D cases is straightforward for the kinetic method.

With the discretization of space x_j, time t^n, and particle velocity u_k, the finite volume scheme based on the integral solution of Eq. (6) is

$$f_{j,k}^{n+1} = f_{j,k}^{n} + \frac{1}{\Delta x}\int \left(u_k \hat{f}_{j-1/2,k} - u_k \hat{f}_{j+1/2,k}\right)dt + \frac{1}{\Delta x}\int\int \frac{g-f}{\tau}dx\,dt, \tag{12}$$

where $f_{j,k}^n$ is the averaged distribution function in the jth-cell $x \in [x_{j-1/2}, x_{j+1/2}]$ at the particle velocity u_k. Instead of using upwinding scheme for the evaluation of the distribution function at a cell interface, the solution $\hat{f}_{j+1/2,k}$ in the above equation is constructed from an integral solution of the BGK model (1) using the method of characteristics [12],

$$\hat{f}_{j+1/2,k} = f(x_{j+1/2}, t, u_k, \xi) = \frac{1}{\tau}\int_{t^n}^{t} g(x', t', u_k, \xi)e^{-(t-t')/\tau}dt' + e^{-(t-t^n)/\tau} f_{0,k}^n\left(x_{j+1/2} - u_k(t-t^n), t^n, u_k, \xi\right), \tag{13}$$

where $x' = x_{j+1/2} - u_k(t-t')$ is the particle trajectory and $f_{0,k}^n$ is the initial gas distribution function of f at time $t = t^n$ around the cell interface $x_{j+1/2}$ at the particle velocity u_k, i.e., $f_{0,k}^n = f_0^n(x, t^n, u_k, \xi)$. In the above equation, $f_{0,k}^n$, is known at the beginning of each time step t^n, and a high-order reconstruction can be used to reconstruct its subcell resolution using TVD and ENO methods. The use of the following discontinuous reconstruction is to introduce artificial dissipation for the unified scheme once the scheme becomes a shock capturing method when the dissipative flow structure cannot be well resolved by the cell size. If the solutions are well resolved, the discontinuous reconstruction will become a continuous one automatically. In order to simplify the notation, in the following the cell interface $x_{j+1/2} = 0$ and $t^n = 0$ are used. For example, around each cell interface $x_{j+1/2}$, at time step t^n the initial distribution function becomes,

$$f_0(x, t^n, u_k, \xi) = f_{0,k}(x, 0) = \begin{cases} f_{j+1/2,k}^l[1 + \sigma_{j,k}x], & x \leqslant 0, \\ f_{j+1/2,k}^r[1 + \sigma_{j+1,k}x], & x > 0, \end{cases} \tag{14}$$

where nonlinear limiter is used to reconstruct $f_{j+1/2,k}^l, f_{j+1/2,k}^r$ and the corresponding slopes $\sigma_{j,k}$. For example, in this paper we will use van Leer limiter in the reconstruction. The cell interface distribution functions become

$$f_{j+1/2,k}^l = f_{j,k} + (x_{j+1/2} - x_j)\sigma_{j,k},$$
$$f_{j+1/2,k}^r = f_{j+1,k} - (x_{j+1} - x_{j+1/2})\sigma_{j+1,k},$$

and

$$\sigma_{j,k} = (\mathrm{sign}(s_1) + \mathrm{sign}(s_2))\frac{|s_1||s_2|}{|s_1| + |s_2|},$$

where $s_1 = (f_{j,k} - f_{j-1,k})/(x_j - x_{j-1})$ and $s_2 = (f_{j+1,k} - f_{j,k})/(x_{j+1} - x_j)$.

There is one-to-one correspondence between an equilibrium state and macroscopic flow variables. For the integral solution of the equilibrium state in Eq. (13), we can first use a continuous particle velocity space to evaluate the integral. For an equilibrium state g around a cell interface ($x_{j+1/2} = 0, t = 0$), same as the BGK-NS scheme, it can be expanded with two slopes [34],

$$g = g_0\left[1 + (1 - H[x])\bar{a}^l x + H[x]\bar{a}^r x + \bar{A}t\right], \tag{15}$$

where $H[x]$ is the Heaviside function defined as

$$H[x] = \begin{cases} 0, & x < 0, \\ 1, & x \geqslant 0. \end{cases}$$

Here g_0 is a local Maxwellian distribution function located at $x = 0$. Even though, g is continuous at $x = 0$, it has different slopes at $x < 0$ and $x \geqslant 0$. In the equilibrium state g, $\bar{a}^l, \bar{a}^r$, and $\bar{A}$ are related to the derivatives of a Maxwellian distribution in space and time. In the above calculation of the equilibrium state in space and time, it is not necessary to use a discretized particle velocity space. Based on the macroscopic flow distributions, we can construct the integral solution with a continuous particle velocity space first, then take its corresponding value at the specific particle velocity when necessary. The expansion of the above equilibrium distribution is coming from a Taylor expansion of a Maxwellian in space and time. In order to have AP scheme for the Navier–Stokes equations, to keep the first-order expansion of an equilibrium state in space and time is

necessary. Certainly, if you would like to increase the order of accuracy or solve Burnett equations as the asymptotic limit in the continuum regime, a high-order expansion needs to be used [15].

The dependence of $\bar{a}^l, \bar{a}^r$ and $\overline{A}$ on the particle velocity can be obtained from a Taylor expansion of a Maxwellian and have the following form,

$$\bar{a}^l = \bar{a}_1^l + \bar{a}_2^l u + \bar{a}_3^l \frac{1}{2}(u^2+\xi^2) = \bar{a}_\alpha^l \psi_\alpha,$$
$$\bar{a}^r = \bar{a}_1^r + \bar{a}_2^r u + \bar{a}_3^r \frac{1}{2}(u^2+\xi^2) = \bar{a}_\alpha^r \psi_\alpha,$$
$$\overline{A} = \overline{A}_1 + \overline{A}_2 u + \overline{A}_3 \frac{1}{2}(u^2+\xi^2) = \overline{A}_\alpha \psi_\alpha,$$

where $\alpha = 1,2,3$ and all coefficients $\bar{a}_1^l, \bar{a}_2^l, \ldots, \overline{A}_3$ are local constants.

The determination of g_0 depends on the determination of the local macroscopic values of ρ_0, U_0 and λ_0 in g_0, i.e.,

$$g_0 = \rho_0 \left(\frac{\lambda_0}{\pi}\right)^{\frac{K+1}{2}} e_0^{-\lambda((u-U_0)^2+\xi^2)},$$

which is determined uniquely using the compatibility condition of the BGK model. Taking the limit $t \to 0$ in Eq. (13) and substituting its solution into Eq. (3), the conservation constraint at $(x = x_{j+1/2}, t = 0)$ gives

$$W_0 = \int g_0 \psi d\Xi = \sum_{k=-N}^{k=N} \left(f_{j+1/2,k}^l H[u_k] + f_{j+1/2,k}^r (1 - H[u_k]) \right) \psi, \tag{16}$$

where $W_0 = (\rho_0, \rho_0 U_0, E_0)^T$ is the conservative macroscopic flow variables located at the cell interface at time $t = 0$. Since $f_{j+1/2,k}^l$ and $f_{j+1/2,k}^r$ have been obtained earlier in the initial distribution function f_0 around a cell interface, the above moments can be evaluated explicitly. Therefore, the conservative variables ρ_0, $\rho_0 U_0$, and E_0 at the cell interface can be obtained, from which g_0 is uniquely determined. Different from the BGK–NS method, the integration of f_0 term in phase space in BGK–NS scheme is replaced by the quadrature formula in particle velocity due to the discretization of phase space. Also, due to the particle velocity discretization, the gas distribution function has more freedom here to recover any shape distribution function in the highly non-equilibrium flow regime, and the macroscopic governing equations underlying the current kinetic approach can be beyond the NS in the general case. For the equilibrium state, λ_0 in g_0 can be found from

$$\lambda_0 = (K+1)\rho_0 \Big/ \left(4\left(E_0 - \frac{1}{2}\rho_0 U_0^2 \right) \right).$$

Then, $\bar{a}^l$ and $\bar{a}^r$ of g in Eq. (15) can be obtained through the relation of

$$\frac{\overline{W}_{j+1}(x_{j+1}) - W_0}{\rho_0 \Delta x^+} = \int \bar{a}^r g_0 \psi d\Xi = \overline{M}_{\alpha\beta}^0 \begin{pmatrix} \bar{a}_1^r \\ \bar{a}_2^r \\ \bar{a}_3^r \end{pmatrix} = \overline{M}_{\alpha\beta}^0 \bar{a}_\beta^r, \tag{17}$$

and

$$\frac{W_0 - \overline{W}_j(x_j)}{\rho_0 \Delta x^-} = \int \bar{a}^l g_0 \psi d\Xi = \overline{M}_{\alpha\beta}^0 \begin{pmatrix} \bar{a}_1^l \\ \bar{a}_2^l \\ \bar{a}_3^l \end{pmatrix} = \overline{M}_{\alpha\beta}^0 \bar{a}_\beta^l, \tag{18}$$

where the matrix $\overline{M}_{\alpha\beta}^0 = \int g_0 \psi_\alpha \psi_\beta d\Xi / \rho_0$ is known, and $\Delta x^+ = x_{j+1} - x_{j+1/2}$ and $\Delta x^- = x_{j+1/2} - x_j$ are the distances from the cell interface to cell centers. Therefore, $(\bar{a}_1^r, \bar{a}_2^r, \bar{a}_3^r)^T$ and $(\bar{a}_1^l, \bar{a}_2^l, \bar{a}_3^l)$ can be found following the procedure as BGK–NS method [34]. In order to evaluate the time evolution part $\overline{A}$ in the equilibrium state, we can apply the following condition

$$\frac{d}{dt} \int (g - \hat{f}) \psi \Xi = 0,$$

at $(x = 0, t = 0)$ [14] and get

$$\overline{M}_{\alpha\beta}^0 \overline{A}_\beta = (\partial\rho/\partial t, \partial(\rho U)/\partial t, \partial E/\partial t)^T = -\frac{1}{\rho_0} \int \left[u(\bar{a}^l H[u] + \bar{a}^r (1 - H[u])) g_0 \right] \psi d\Xi. \tag{19}$$

Up to this point, we have determined all parameters in the initial gas distribution function f_0 and the equilibrium state g in space and time locally. After substituting Eq. (14) and (15) into Eq. (13) and taking $u = u_k$ in g_0, $\bar{a}^l, \bar{a}^r$ and $\overline{A}$, the gas distribution function $\hat{f}(x_{j+1/2}, t, u_k, \xi)$ at the discretized particle velocity u_k can be expressed as

$$\begin{aligned} \hat{f}_{j+1/2,k}(0,t) = {} & (1 - e^{-t/\tau}) g_0 + \left(\tau(-1 + e^{-t/\tau}) + t e^{-t/\tau} \right) (\bar{a}^l H[u_k] + \bar{a}^r (1 - H[u_k])) u_k g_0 + \tau \left(t/\tau - 1 + e^{-t/\tau} \right) \overline{A} g_0 \\ & + e^{-t/\tau} \left((1 - u_k t \sigma_{j,k}) H[u_k] f_{j+1/2,k}^l + (1 - u_k t \sigma_{j+1,k})(1 - H[u_k]) f_{j+1/2,k}^r \right) \triangleq \tilde{g}_{j+1/2,k} + \tilde{f}_{j+1/2,k}, \end{aligned} \tag{20}$$

where $\tilde{g}_{j+1/2,k}$ is all terms related to the integration of the equilibrium state g and $\tilde{f}_{j+1/2,k}$ is the terms from initial condition f_0. The collision time τ in the above distribution function is determined by $\tau = \mu(T_0)/p_0$, where T_0 is the temperature and p_0 is the pressure, and both of them can be evaluated from W_0 at the cell interface. The above time-accurate gas distribution function can be used in Eq. (12) for the fluxes at a cell interface.

In order to discretize the collision term in Eq. (12) efficiently and accurately, a multiscale unified formulation is the following. Let's first take moment ψ on Eq. (12). Due to the vanishing of the particle collision term for the conservative variables, we have

$$W_j^{n+1} = W_j^n + \frac{1}{\Delta x}\int\int_{t^n}^{t^{n+1}} u(\tilde{g}_{j-1/2} - \tilde{g}_{j+1/2})\psi dt d\Xi + \frac{1}{\Delta x}\sum_k \int_{t^n}^{t^{n+1}} u_k\left(\tilde{f}_{j-1/2,k} - \tilde{f}_{j+1/2,k}\right)\psi dt, \tag{21}$$

where $\tilde{g}_{j+1/2}$ has the same expression as $\tilde{g}_{j+1/2,k}$, but is integrated in a continuous particle velocity space $u_k = u$. The integration of the equilibrium part $\tilde{g}$ can be evaluated exactly and the integration of the non-equilibrium part $\tilde{f}$ can be done using the quadrature. For the update of the conservative variables, the difference between the above formulation and the BGK–NS scheme is that the discrete sum is used for the integration of the initial distribution function f_0 in particle velocity space. For a highly non-equilibrium flow, the real distribution function f_0 can be a complicated function, and a discretization of particle velocity space has to be used. For the original BGK–NS scheme targeting on the NS solutions [34], the initial gas distribution function f_0 can be reconstructed from the distribution of macroscopic variables according to the Chapman–Enskog expansion. Therefore, the specific form of initial condition f_0 can be mathematically reconstructed. In the continuum flow limit, due to the sufficient number of particle collisions and with the condition of time step being much larger than the particle collision time, the contribution of the integration of the equilibrium state $\tilde{g}_{j+1/2}$ will be dominant in the final solution of the distribution function $\tilde{f}_{j+1/2,k}$. The $\tilde{g}_{j+1/2}$ itself gives a corresponding NS distribution function [33], and the contribution from initial term $\tilde{f}_{j+1/2,k}$ vanishes. As a result, the updated discrete form of the distribution function $f_{j,k}^{n+1}$ will present a Chapman–Enskog NS distribution function. Therefore, in the continuum flow regime, the BGK–NS scheme with continuous particle velocity space and the current unified method with discretized particle velocity space will become the same scheme. In the continuum flow regime, for the NS solutions the update of the conservative variables through the above Eq. (21) is enough, because the gas distribution function $f_{j,k}^{n+1}$ can be reconstructed from the updated conservative variables. Therefore, for the continuum flow only, like the BGK–NS scheme [34], we do not basically update the gas distribution function. This also illustrates that in terms of the conservative flow variable update, the unified scheme is an AP method in the continuum limit. However, the unified scheme is not limited to continuum flow. In the highly non-equilibrium flow regime, Eq. (21) for the update of conservative variables is still correct. For example, in the collisionless limit, the non-equilibrium part $\tilde{f}_{j-1/2,k}$ and $\tilde{f}_{j+1/2,k}$ will take dominant effect, and the contribution from the equilibrium part vanishes. Therefore, the unified scheme has the correct collisionless limit as well.

In general, based on the above updated conservative variables, we can immediately obtain the equilibrium gas distribution function $g_{j,k}^{n+1}$ inside each cell, therefore based on Eq. (12) the unified kinetic scheme for the update of gas distribution function becomes

$$f_{j,k}^{n+1} = f_{j,k}^n + \frac{1}{\Delta x}\left(\int_{t^n}^{t^{n+1}} u_k(\tilde{g}_{j-1/2,k} - \tilde{g}_{j+1/2,k})dt + \int_{t^n}^{t^{n+1}} u_k\left(\tilde{f}_{j-1/2,k} - \tilde{f}_{j+1/2,k}\right)dt\right) + \frac{\Delta t}{2}\left(\frac{g_{j,k}^{n+1} - f_{j,k}^{n+1}}{\tau^{n+1}} + \frac{g_{j,k}^n - f_{j,k}^n}{\tau^n}\right), \tag{22}$$

where trapezoidal rule has been used for the time integration of collision term. So, from the above equation, the unified multiscale scheme for the update of gas distribution function is

$$f_{j,k}^{n+1} = \left(1 + \frac{\Delta t}{2\tau^{n+1}}\right)^{-1}\left[f_{j,k}^n + \frac{1}{\Delta x}\left(\int_{t^n}^{t^{n+1}} u_k(\tilde{g}_{j-1/2,k} - \tilde{g}_{j+1/2,k})dt + \int_{t^n}^{t^{n+1}} u_k\left(\tilde{f}_{j-1/2,k} - \tilde{f}_{j+1/2,k}\right)dt\right) + \frac{\Delta t}{2}\left(\frac{g_{j,k}^{n+1}}{\tau_j^{n+1}} + \frac{g_{j,k}^n - f_{j,k}^n}{\tau_j^n}\right)\right], \tag{23}$$

where no iteration is needed for the update of the above solution. The particle collision times τ_j^n and τ_j^{n+1} are defined based on the temperature and pressure in the cell, i.e., $\tau_j^n = \mu(T_j^n)/p_j^n$ and $\tau_j^{n+1} = \mu(T_j^{n+1})/p_j^{n+1}$, which are known due to the update of macroscopic flow variables in Eq. (21).

4. Physical and numerical analysis

In the previous section, we present a unified kinetic scheme based on the kinetic BGK model. The scheme is a natural extension of BGK–NS scheme for the NS solutions to the rarefied flow regimes with discretized particle velocity space. The scheme can be further understood in the following aspects.

4.1. Dynamic hybrid method

The unified scheme is a multiscale hybrid method with both macroscopic and microscopic variable updates. The traditional hybrid approach is based on a geometrical one. In different flow regions, different governing equations are solved. At the same time, different patches are connected through buffer zone. However, instead of solving different governing

equations as most hybrid schemes do, we couple them in the way of evaluating the flux function across the cell interface. In the continuum flow regime, the intensive particle collision will drive the system close to equilibrium state. Therefore, the part based on the integration of equilibrium state $\tilde{g}_{j+1/2,k}$ in Eq. (20) at the cell interface will automatically take a dominant role. It can be shown that in smooth flow region $\tilde{g}_{j+1/2,k}$ gives precisely the NS gas distribution function. Since there is one-to-one correspondence between macroscopic flow variables and the equilibrium distribution, the integration of the equilibrium part can be also fairly considered as the macroscopic composition part of the scheme. In the free molecule limit with inadequate particle collisions, the integral solution at the cell interface will automatically present a purely upwinding scheme, where the particle transport from $\tilde{f}_{j+1/2,k}$ will be the main part. Therefore, the scheme captures the flow physics in the collisionless limit as well. This unified approach can be considered as a dynamic hybrid method instead of geometrical one. The reason for most other approaches to use a geometrical way is due to the fact that their flux functions across a cell interface are solely based on the kinetic upwinding discretization, i.e., the so-called $\tilde{f}_{j+1/2,k}$ term in Eq. (20). As we know, the kinetic upwinding is only correct in the collisionless or highly non-equilibrium regime. Therefore, in the traditional hybrid scheme, the computational domain has to be divided into equilibrium and non-equilibrium flow regions. Physically this kind of geometrical division is artificial and there should have no region where both approaches are applicable, because the above two approaches have significant dynamic differences in their flux evaluation. In the unified method, a single computation domain is used and the dynamic differences in the particle behavior is obtained by solving the full approximate Boltzmann equation, which is valid all the way from the continuum to rarefied flows. Certainly, in order to save computational time we may also develop a hybrid method which uses the current unified scheme as a non-equilibrium flow solver and adopts the BGK–NS method as a continuum flow solver. In the continuum flow regime, this kind of hybrid scheme is actually a scheme which is different from the unified method only by simply replacing the discretized particle distribution function f_0 of Eq. (14) by a distribution function f_0 of the Chapman–Enskog NS-type with a continuous particle velocity space [34].

4.2. Asymptotic preserving property

Asymptotic preserving for the NS solution in the continuum limit is a preferred property for the kinetic scheme. In order to design an AP method which is valid for both NS equations and the free molecule limit, it is necessary to solve the full BGK Eq. (1) for the flux evaluation in Eq. (6) across a cell interface. The necessity of using the above equation can be understood in the following. First, let's forget about numerical mesh. Since the Boltzmann equation couples the particle transport and collision everywhere, at any point in space and time (x,t), both collision and transport exist. For example, $uf_x(x,t)$ and $(g-f)/\tau$ are continuous functions of x and t. When evaluating particle transport across a cell interface, dynamically all particles in a small domain around the cell interface will effect the particle evolution through transport and collision. In other words, those molecules passing through cell interface do suffer from particle collisions as well. The collisionless or upwinding discretization which accounts only for $\tilde{f}_{j+1/2,k}$ term in Eq. (20) is physically incorrect.

As shown in the last section, the distinguishable point of the current scheme is that the collisional BGK is solved for the flux evaluation at a cell interface. In the continuum flow regime, only conservative flow variables are concerned. The flux evaluation for the conservative variables update in Eq. (21) is simply a discretized version of the BGK–NS method for the NS equations. For the unified scheme, for the continuum flow, we can use the time step which is much larger than the particle collision time, i.e., $\Delta t \gg \tau$. In this case, the distribution function for the flux evaluation at the cell interface Eq. (20) will become

$$f_{j+1/2}(t) = g_0\Big(1 - \tau(\bar{a}u + \overline{A}) + t\overline{A}\Big), \tag{24}$$

which is exactly the Chapman–Enskog expansion of the NS solution [34] with $\bar{a} = \bar{a}^l H[u_k] + \bar{a}^r(1 - H[u_k])$. In other words, in the continuum limit, the integral solution from the equilibrium state is dominant, and the updating of the macroscopic flow variables follow the NS solutions. So, the unified scheme provides an accurate NS solutions in the update of the conservative variables inside each cell. The unified scheme is an AP method and its accuracy in the continuum flow regime is $O(\tau(\Delta t)^2)$ [21,23]. Theoretically, in the continuum limit it is not necessary to evaluate the distribution function anymore. If a simple upwinding method is used for the flux evaluation through $\tilde{f}_{j+1/2,k}$, as done by most kinetic methods, an artificial viscosity term being proportional to time step Δt will be introduced in its governing equations. So, in this case, the kinetic scheme can only become an asymptotic preserving method for the Euler equations.

4.3. Determination of time step

In the continuum limit, for the unified scheme the time step is determined by the CFL condition,

$$\Delta t = \mathrm{CFL}\frac{\Delta x}{|U| + c},$$

where CFL is the CFL number and c is the sound speed. On the other hand, the particle collision time is defined by

$$\tau = \frac{\mu}{p} = \frac{\rho|U|\Delta x}{pRe},$$

where $Re = \rho\Delta x|U|/\mu$ is the cell's Reynolds number. With the approximation,

$$|U| + c \simeq c,$$

which is true for low speed flow and is approximately correct even for hypersonic flow because the flow velocity is on the same order of sound speed, we have

$$\frac{\Delta t}{\tau} = \frac{Re}{M},$$

where M is the Mach number. So, for the continuum flow computation, even for a modest cell Reynolds number, such as 10^4, the time step for the unified scheme can be several order larger than the particle collision time. The above equation can be also written in the following form

$$\Delta t = \frac{\tau}{\mathrm{Kn}}, \tag{25}$$

where $\mathrm{Kn} = M/Re$ is the local cell Knudsen number. So, for a flow with all Knudsen regimes from the continuum to free molecules, such as the nozzle flows, the overall time step taken by the unified scheme can be the one which maximizes the above time step. As a result, the time step Δt used in the whole domain will be $\Delta t \gg \tau$ in the continuum and $\Delta t < \tau$ in rarefied regimes. In comparison with the schemes which use a time step solely controlled by the mininum particle collision time, the current unified scheme is much more efficient.

4.4. Prandtl number fix

The unified scheme is based on the BGK model, which presents unit Prandtl number. For real gas, due to the interaction forces between molecules, the Prandtl number is approximately equal to 2/3 for a monatomic gas. In order to extend the unified scheme to simulate flow with any realistic Prandtl number, the heat flux in the scheme has to been modified. Traditionally, in order to fix the Prandtl number, many approaches have been investigated. The well-known ones include Ellipsoid BGK model, velocity dependent particle collision time, and Shakhov model [19,28,16]. Since the heat flux is a macroscopic flow variable, it is related to the collective flow properties, it is very hard to directly modify it in the update of gas distribution function. Fortunately, the current unified scheme is a multiscale method. Both microscopic distribution function and macroscopic conservative flow variables are updated in the scheme. As a result, similar to the BGK–NS method [34], in the process of updating conservative flow variables, we can modify the heat flux across the cell interface in Eq. (21) in the following way. In the flux evaluation in Eq. (21), the interface flux is given by

$$F_{j+1/2} = \int u\tilde{g}_{j+1/2}\psi d\Xi + \sum_k u_k\tilde{f}_{j+1/2,k}\psi, \tag{26}$$

which include the energy flux F_E. Therefore, the easiest way to modify the Prandtl number is to change the heat flux. The heat flux at a cell interface is

$$q_{j+1/2} = \int \frac{1}{2}(u - U_{j+1/2})\left((u - U_{j+1/2})^2 + \xi^2\right)\psi\tilde{g}_{j+1/2}d\Xi + \sum_k \frac{1}{2}(u_k - U_{j+1/2})\left((u_k - U_{j+1/2})^2 + \xi^2\right)\psi\tilde{f}_{j+1/2,k}, \tag{27}$$

where the interface averaged flow velocity is defined by

$$U_{j+1/2} = \left(\int u\tilde{g}_{j+1/2}d\Xi + \sum_k u_k\tilde{f}_{j+1/2,k}\right) \Big/ \left(\int \tilde{g}_{j+1/2}d\Xi + \sum_k \tilde{f}_{j+1/2,k}\right).$$

So, with a given Prandtl number Pr, we only need to replace the original energy flux F_E in Eq. (26) by the new one

$$F_E^{new} = F_E + \left(\frac{1}{Pr} - 1\right)q_{j+1/2}.$$

With the correct Prandtl number in the updated macroscopic variables, subsequently it effects the construction of the equilibrium state g^{n+1} at the next level. Therefore, the update of microscopic gas distribution function in Eq. (23) is modified as well. The above procedure of the modification of heat flux has some similarity with the DSMC method. For example, in the current scheme the post-collision particle velocity and directions are controlled through the modified g^{n+1}. The effectiveness of the above Prandtl number fix will be tested in the next section in the shock structure calculations.

4.5. Collisionless limit

In the free molecule limit, i.e., $\tau \to \infty$, the unified scheme becomes

$$f_{j,k}^{n+1} = f_{j,k}^n - \frac{1}{\Delta x}\int_{t^n}^{t^{n+1}} u_k\left(\hat{f}_{j-1/2,k} - \hat{f}_{j+1/2,k}\right)dt,$$

where only the initial term f_0 in the integral solution of the BGK model (13) remains, and

$$\hat{f}_{j+1/2,k}(x,0) = \begin{cases} f^l_{j+1/2,k}[1 - u_k t\sigma_{j,k}], & u_k \geqslant 0, \\ f^r_{j+1/2,k}[1 - u_k t\sigma_{j+1,k}], & u_k < 0, \end{cases}$$

The above equation is a purely free molecule transport equation. So, in this limit the unified kinetic scheme is a valid one.

5. Numerical experiments

The development of accurate kinetic methods for simulating flows in entire Knudsen number regime is difficult. The discrete ordinate methods (DOM) of Yang–Huang, Mieussens, and Li–Zhang [38,18,16] are accurate numerical methods in all Knudsen numbers, but the limitation of the time step on these schemes in the continuum flow regime makes them impossible to be applied in computations. But, still the results from DOM methods can be used as a benchmark solution for these flows if the computational cost is affordable. This is also true for many other kinetic methods, such as DSMC and direction Boltzmann solver [4,1].

In this section, in order to test the unified scheme we are going to present four one-dimensional test cases from free molecule flow to continuum Euler and NS solutions. The flow features of different local Knudsen numbers will be covered. In this section, we are going to test three schemes, which are the unified scheme (unified BGK), discrete ordinate method (BGK-DOM) [38], and the continuum flow solver BGK–NS for NS solutions [34]. The unified scheme will be applied to all Knudsen number flow regime. BGK–DOM will be applied to rarefied and near continuum flows where it is applicable. The BGK–NS will be applied to near continuum and continuum flows. For the unified BGK method, in most test cases the time step is determined by the CFL condition with CFL number 0.9. For the BGK–DOM, the time step is limited by the particle collision time,

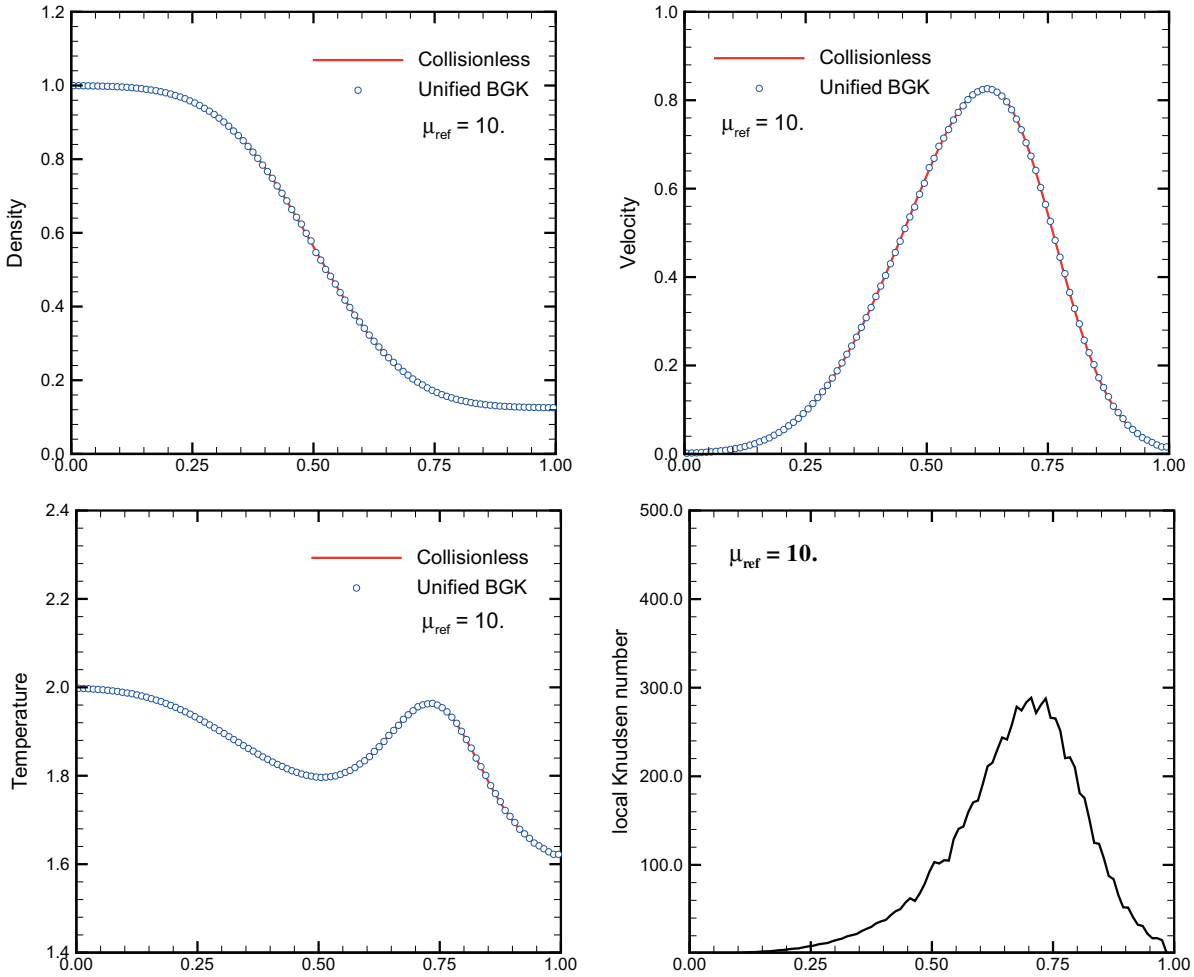

Fig. 1. Sod test: unified BGK and exact collisionless Boltzmann solutions at $\mu_{ref} = 10$. All x-coordinates and physical quantities are dimensionless.

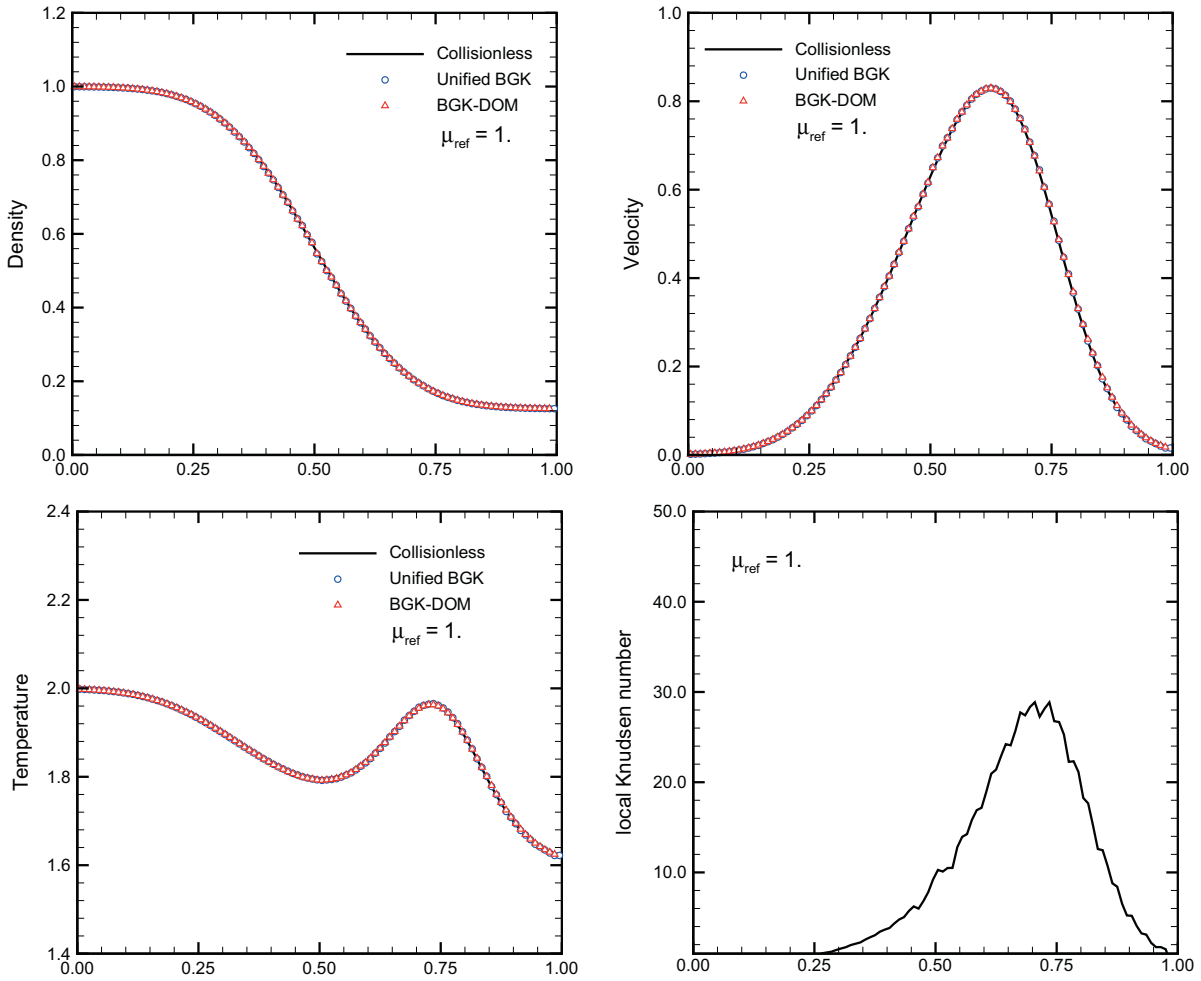

Fig. 2. Sod test: unified BGK, BGK-DOM, and collisionless Boltzmann solutions at $\mu_{ref} = 1$. All x-coordinates and physical quantities are dimensionless.

which is on the order of $\Delta t \leqslant 2\tau_m$, where τ_m is the minimum particle collision time in the domain. For the BGK–NS code, the time step is also determined by the CFL condition.

Case (1). From free molecule to Euler solutions

The first case is the standard Sod test. In the computational domain $x \in [0,1]$, 100 cells with uniform mesh in space are used. In the particle velocity space, 200 points with uniform distribution are used. The main purpose of this paper is to test the idea instead of optimizing the velocity space. So, a large number of velocity grid points is used. The initial condition for the mass density, velocity, and pressure is

$$(\rho_l, U_l, p_l) = (1.0, 0.0, 1.0), \quad x \leqslant 0.5,$$
$$(\rho_r, U_r, p_r) = (0.125, 0.0, 0.1), \quad x > 0.5.$$

The reference mean free path ℓ_{mfp} is evaluated by reference state with $p_{ref} = 1.0$, $\rho_{ref} = 1.0$, and the viscosity coefficient μ_{ref}, which is defined by

$$\ell_{mfp} = \frac{16}{5\sqrt{2\pi}} \frac{\mu_{ref}}{\sqrt{\rho_{ref} p_{ref}}}.$$

So, the local mean free path in the gas becomes

$$\ell_{local} = \frac{\mu}{\mu_{ref}} \sqrt{\frac{\rho_{ref}}{\rho} \frac{p_{ref}}{p}} \ell_{mfp},$$

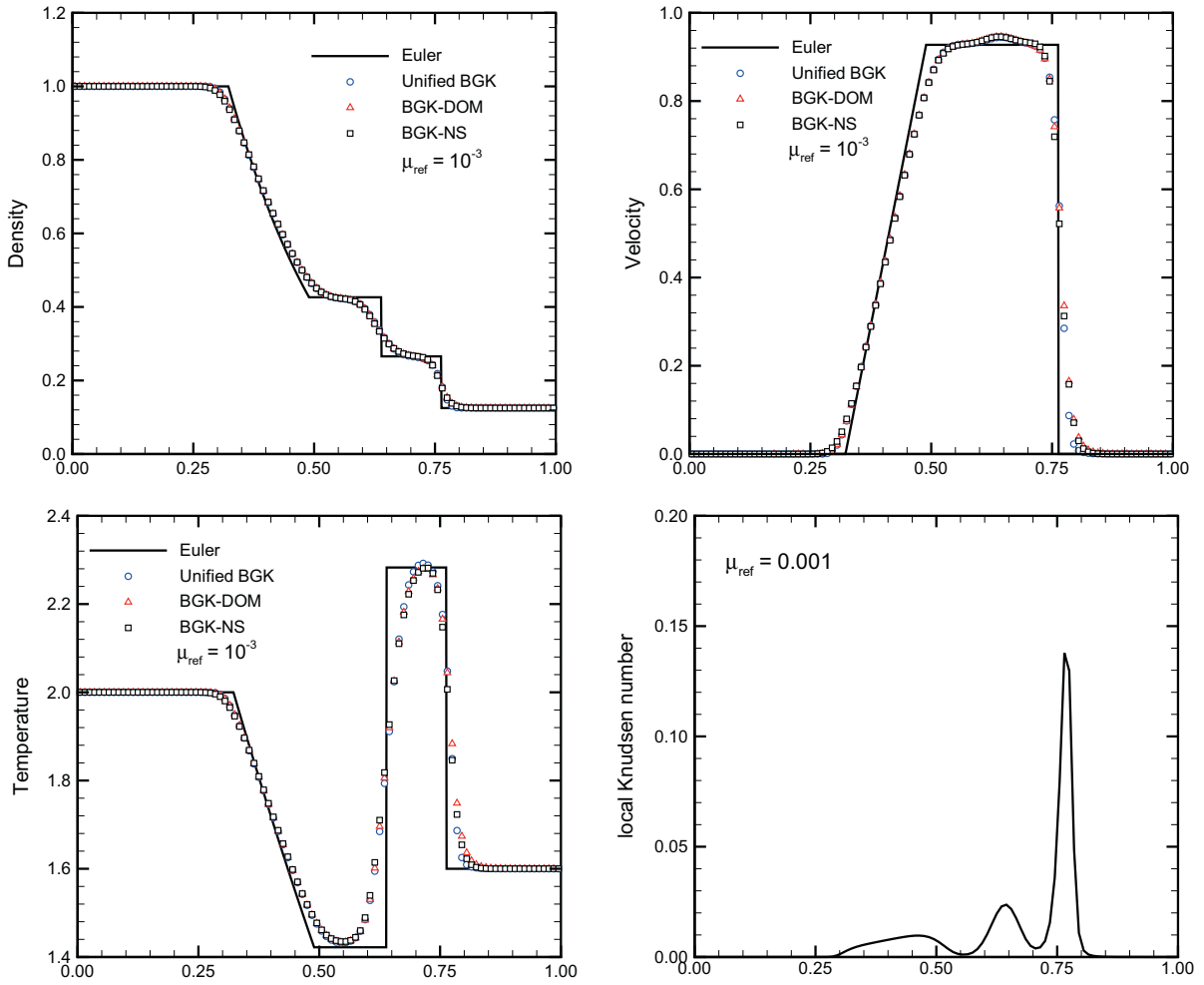

Fig. 3. Sod test: unified BGK, BGK-DOM, BGK-NS, and Euler solutions at $\mu_{ref} = 10^{-3}$. All x-coordinates and physical quantities are dimensionless.

where $\mu = \sqrt{\frac{p}{p_{ref}}\frac{\rho_{ref}}{\rho}}\mu_{ref}$ is determined as hard sphere molecules. For the Sod test case, the initial mean free path of the left state is equal to the reference mean free path, and the mean free path of the right side gas is about nine times that of the left state. With the variation of μ_{ref}, we can basically simulate flows with different degree of rarefaction. The output time for all simulations is $t = 0.15$. In the simulating cases with a variable reference viscosity coefficients $\mu_{ref} = 10, 1.0, 10^{-3}$, and 10^{-5}, and the corresponding mean free path for the left state of the Sod test become $12.77, 1.277, 1.277 \times 10^{-3}$, and 1.277×10^{-5}, which cover the flows from free molecule to continuum one in terms of the size of the computational domain. A useful parameter is the local flow Knudsen number, which is defined by

$$Kn_{local} = \frac{\ell_{local}}{\rho}\frac{d\rho}{dx}.$$

For example, for the case of $\mu_{ref} = 1.0$, the local mean free path is much greater than 1. So, with the unit length of computational domain, the flow is basically a free molecule one.

Fig. 1 shows the simulation results of density, velocity, temperature, and Knudsen number for the case with $\mu_{ref} = 10$. As shown in the Knudsen number plot, it is basically the free molecule flow. The results from the unified BGK precisely recovers the exact solution of the collisionless Boltzmann equation. Fig. 2 shows the same calculation at $\mu_{ref} = 1.0$, where the collisionless, unified BGK, and BGK–DOM results are plotted. From the local Knudsen number plot, it is obvious that most part of the flow is still in the collisionless regime. At $\mu_{ref} = 10^{-3}$, the flow is near continuum regime. Fig. 3 shows the solutions from all three schemes, which are unified BGK, BGK–DOM, and BGK–NS. Since the BGK–NS is an accurate Navier–Stokes flow solver for the linear dissipative contact wave [34,36,37], its solution can be used as a benchmark NS solution. Fig. 3 clearly shows that unified BGK and BGK–DOM can get the NS solution as well. However, for the nonlinear shock front with $Kn \simeq 0.1$, all three schemes have no enough resolution to resolve the shock structure. As μ_{ref} gets to 10^{-5}, the flow is basically in the continuum regime. It becomes impossible for BGK–DOM method to get solution due to its computational cost. So, Fig. 4 shows

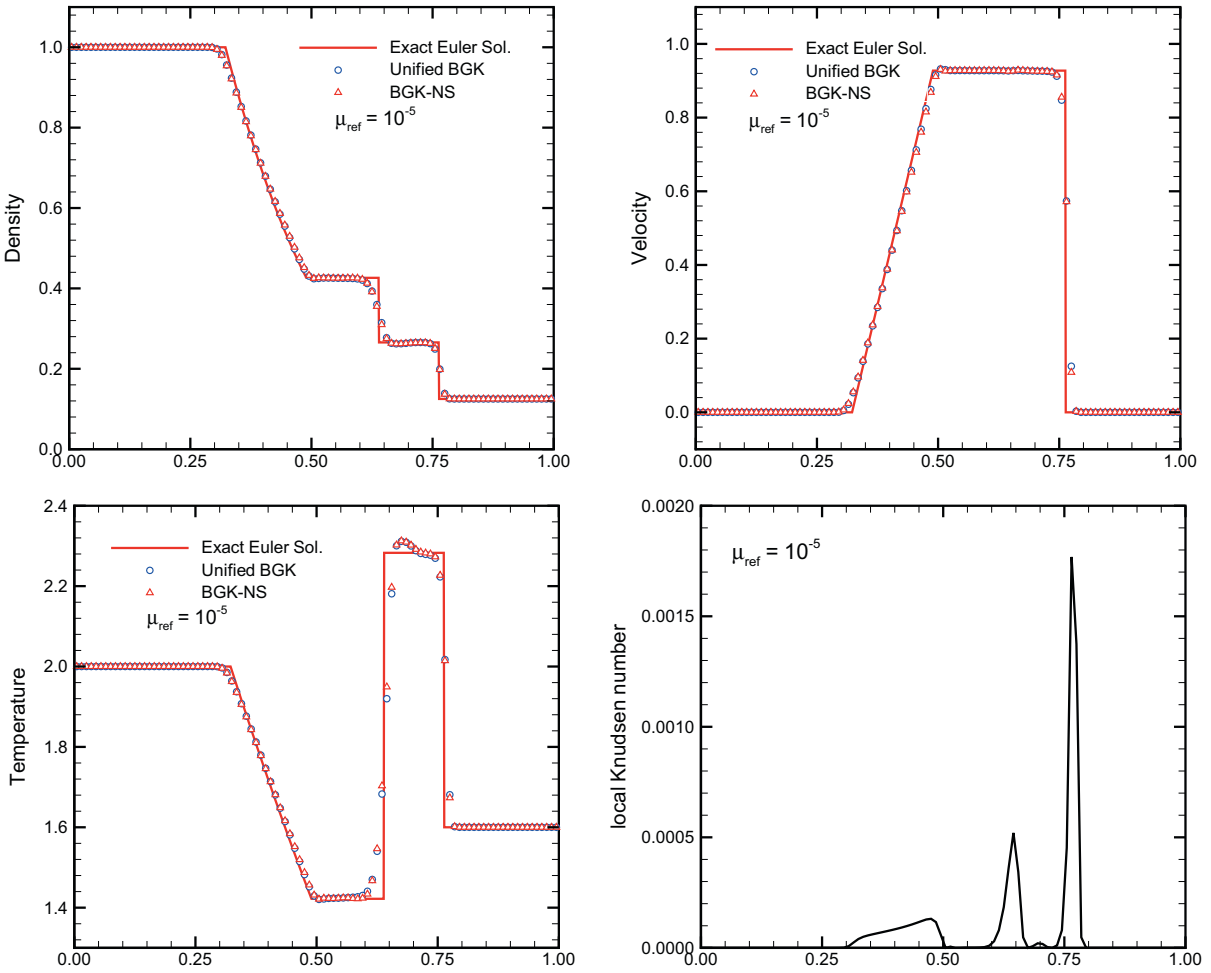

Fig. 4. Sod test: unified BGK, BGK-NS, and Euler solutions at $\mu_{ref} = 10^{-5}$. All x-coordinates and physical quantities are dimensionless.

the solutions from unified BGK and BGK–NS only. In this case, unified BGK basically becomes a shock capturing scheme for the Euler solution because the numerical mesh size cannot resolve the physical structure at all. In the under-resolved case, there is obvious numerical oscillation from both BGK–NS and unified BGK schemes at the contact wave. The reason for the oscillation may be due to the nonlinear limiter used in the scheme. The BGK–NS scheme uses nonlinear limiter on the conservative variables directly in the initial data reconstruction, and the unified BGK uses that on the discretized gas distribution function. It seems that if characteristics variables are used for the initial reconstruction for the BGK–NS scheme, the oscillation can be reduced. Using different flow variables in the reconstruction is basically to redistribution the total energy into kinetic and thermal ones differently [34].

Case (2). Upper and Lower transition flow regimes

The second test case is designed as a case which covers flow in the upper and lower transition regimes. The purpose is to show the efficiency of unified BGK and BGK–DOM method. The computational domain is $x \in [0,2]$ with different number of mesh points. The output time for all simulations is $t = 0.1$. The initial condition for this case

$$\begin{aligned}
&(\rho_l, u_l, p_l) = (0.001, 0.0, 0.001), \quad x \leqslant 0.8,\\
&(\rho_m, u_m, p_m) = (10.0, 0.0, 10.0), \quad 0.8 < x \leqslant 1.2,\\
&(\rho_r, u_r, p_r) = (0.001, 0.0, 0.001), \quad 1.2 < x \leqslant 2.0.
\end{aligned} \tag{28}$$

We have tested this case with two reference viscosity coefficients $\mu_{ref} = (10^{-3}, 10^{-4})$. The mean free path in the central region and two sides are $(1.27 \times 10^{-4}, 1.27 \times 10^{-5})$ and $(1.27, 0.127)$ separately. The corresponding collision times are $(1.0 \times 10^{-4}, 1)$ and $(1.0 \times 10^{-5}, 0.1)$. Therefore, the flows are basically in the upper and lower transition regimes. In this calculation, for the BGK–DOM method, the time step is limited to $\Delta t \leqslant 2\tau_m$, where τ_m is the minimum particle collision time. For the unified scheme, the time step is determined by the CFL condition. As we know, BGK–DOM method is actually an

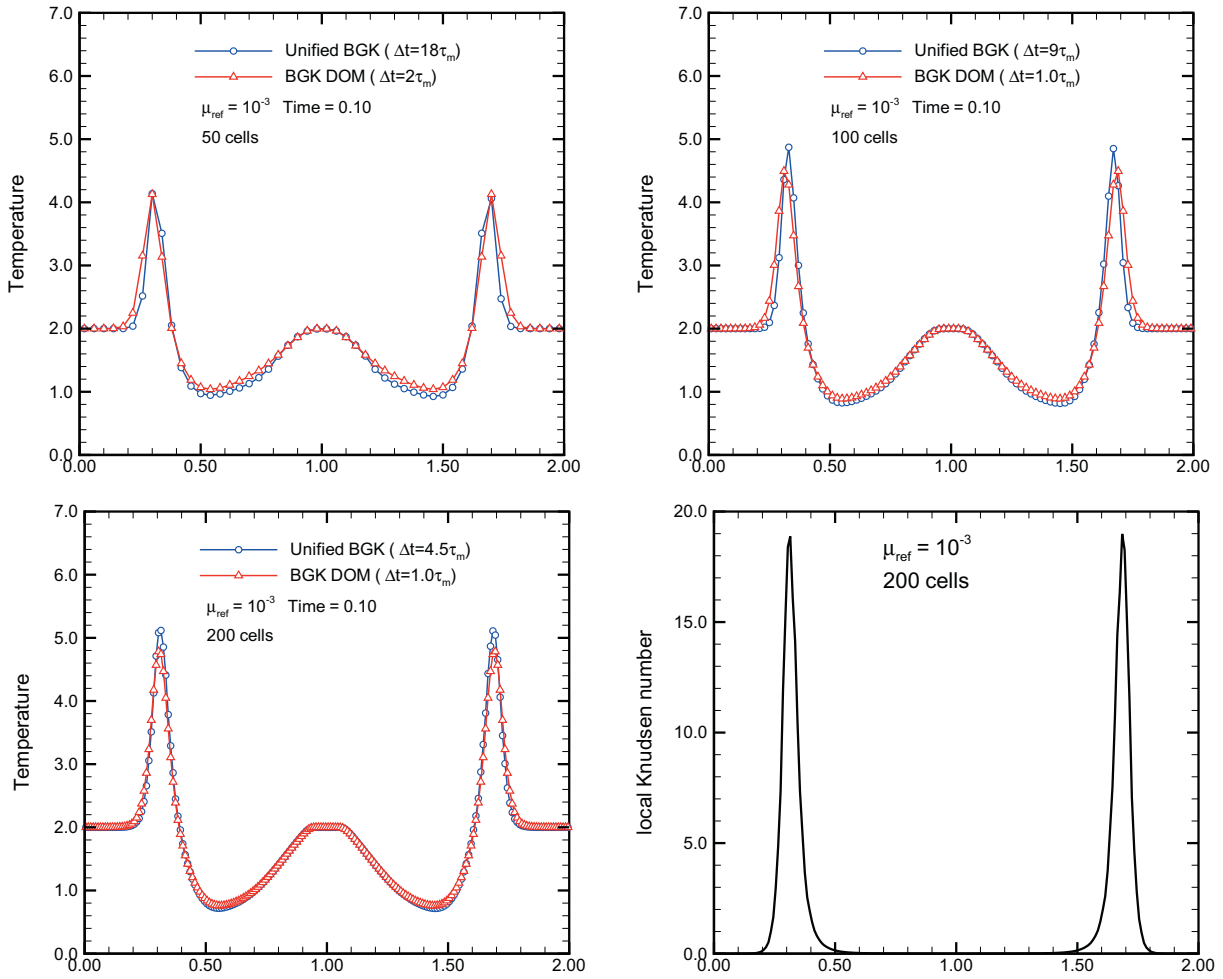

Fig. 5. Test: unified BGK and BGK-DOM solutions with different mesh size and time steps at $\mu_{ref} = 10^{-3}$. All x-coordinates and physical quantities are dimensionless.

accurate flow solver in all Knudsen number regime. The problem for it is that the time step is limited and the scheme will become extremely expensive in the continuum limit. In the following test, we would like to show that the unified scheme can present accurate solutions as well with a much larger time step. Also, in order to test the sensitivity of the solution on the numerical mesh size, three meshes with 50, 100 and 200 will be used in the domain. The first one is about the upper transition flow calculation with $\mu_{ref} = 10^{-3}$. Fig. 5 shows the temperature and local Knudsen number distributions by the unified scheme and BGK–DOM in three different mesh sizes. As shown in the figure, with the similar solution the unified scheme can use a larger time step, which is on the order of 10 times. In the lower transition regime with $\mu_{ref} = 10^{-4}$, Fig. 6 presents temperature and local Knudsen number distributions with three different mesh sizes. As shown, the unified scheme can use a time step which is on the order of 100 times larger than the time step used in BGK–DM method. For the continuum high Reynolds number flows, the reference viscosity coefficients can be on the order of 10^{-5}, 10^{-6}. Under these conditions, the BGK–DOM method is computationally prohibitive due to its extreme cost. However, under these conditions the time step used by the unified scheme can be 10^4, 10^5 times larger than the BGK–DOM time step. Also, in the continuum flow regime, the unified scheme will converge to the BGK–NS solution, where the Navier–Stokes solutions can be confidently obtained. However, in the highly non-equilibrium regime with local $Kn > 1$, both unified and DOM schemes need to use a time step which is less than the particle collision time. Under these situation, the unified and DOM schemes are similar and there is no obvious advantage to use unified method.

Case (3). Shock structure tests

The following test cases are related to the shock structure calculation with low and high Mach numbers. The purpose of these tests are two folds. First, the shock structure calculation does not involve any boundary condition. The effect from the physical modeling in the scheme can be clearly observed. Second, there are abundant experimental and numerical solutions

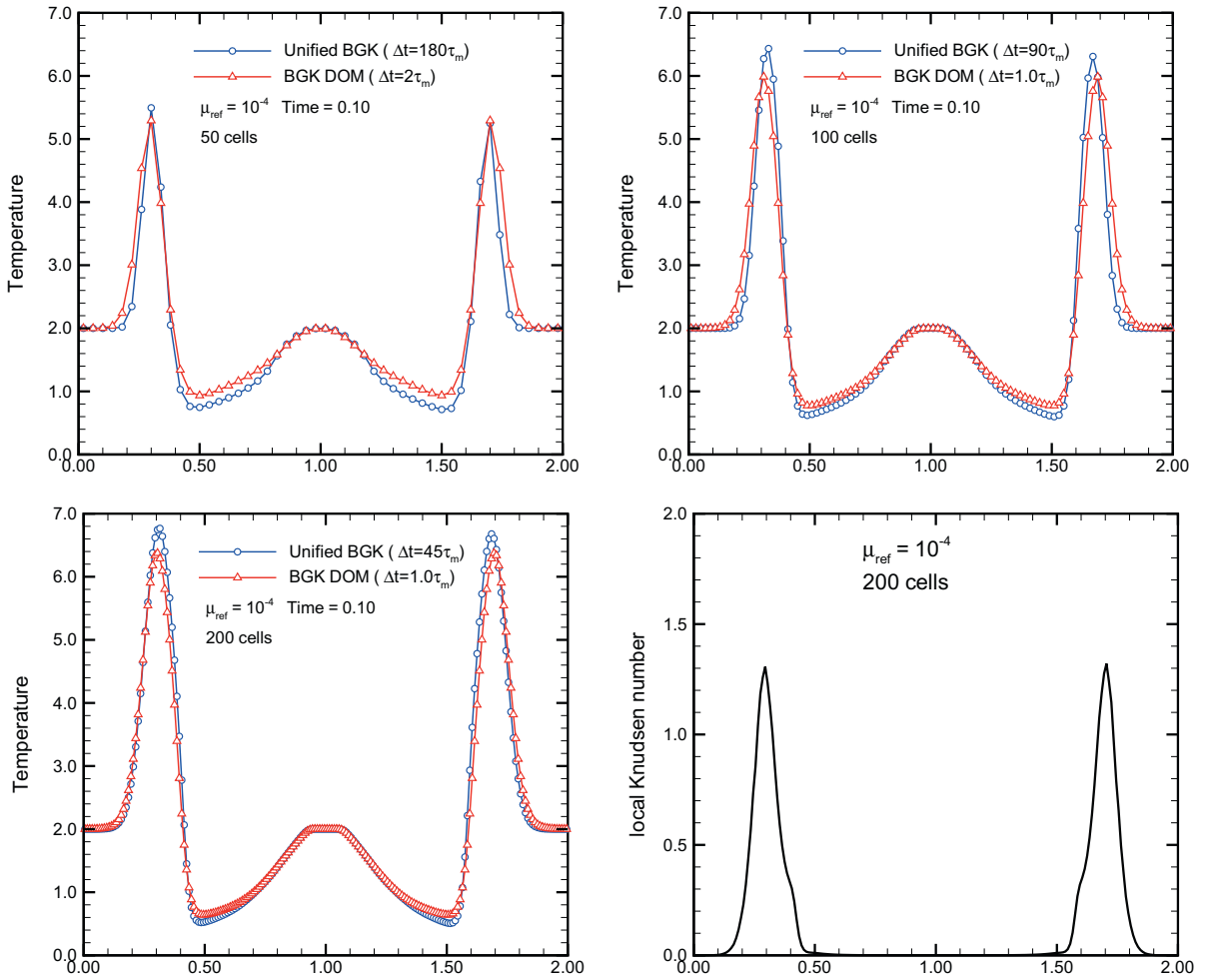

Fig. 6. Test: unified BGK and BGK-DOM solutions with different mesh size and time step at $\mu_{ref} = 10^{-4}$. All x-coordinates and physical quantities are dimensionless.

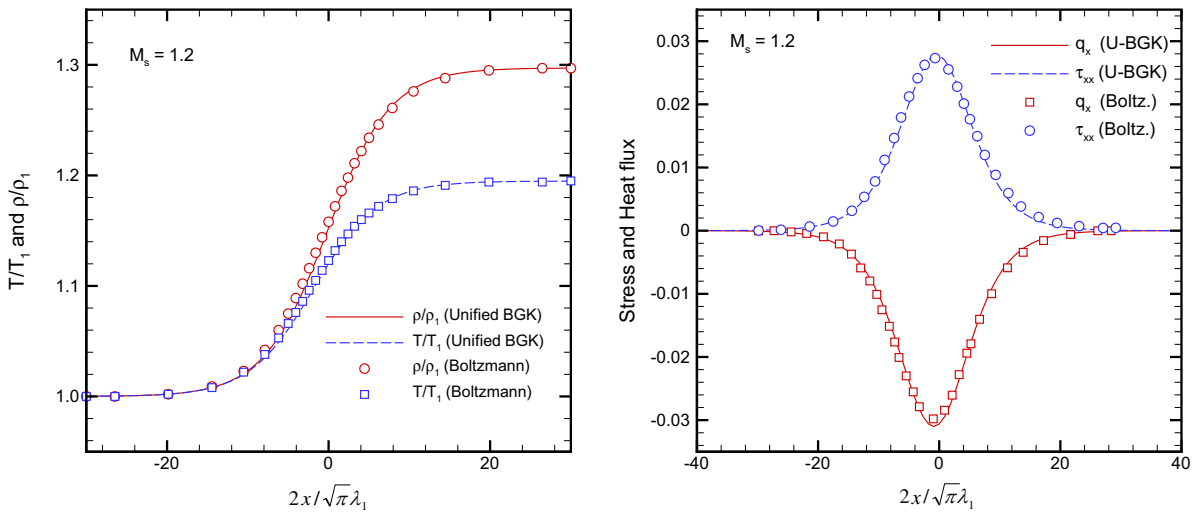

Fig. 7. Unified BGK for $M = 1.2$ shock structure calculation. Left: density and temperature distributions. Right: stress and heat flux. The reference solution is from the solution based on the Boltzmann equation [20].

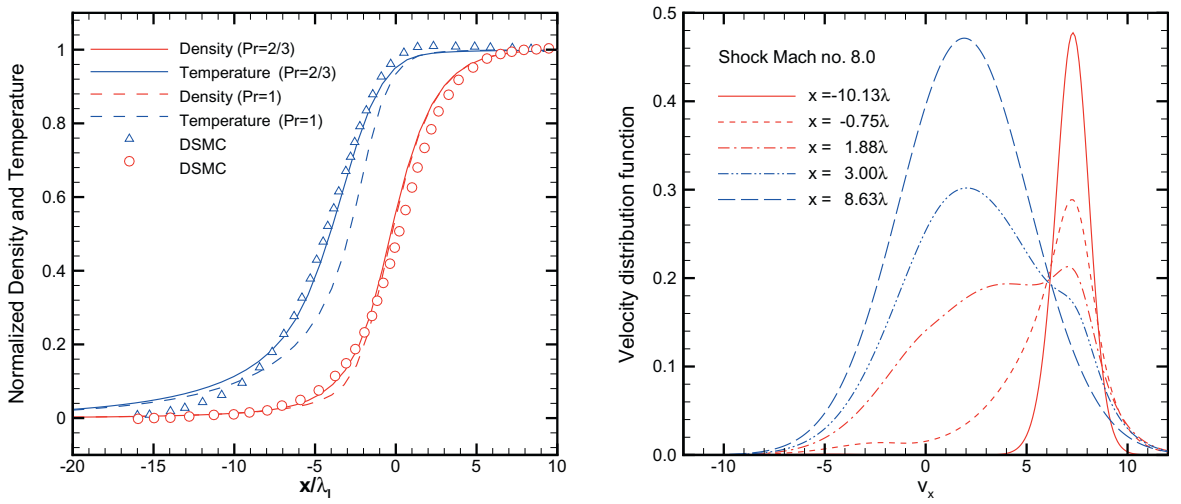

Fig. 8. Unified BGK for $M = 8$ shock structure calculation. Left: density and temperature distributions. Right: gas distribution functions inside the shock layer. The reference solution is from the DSMC [4].

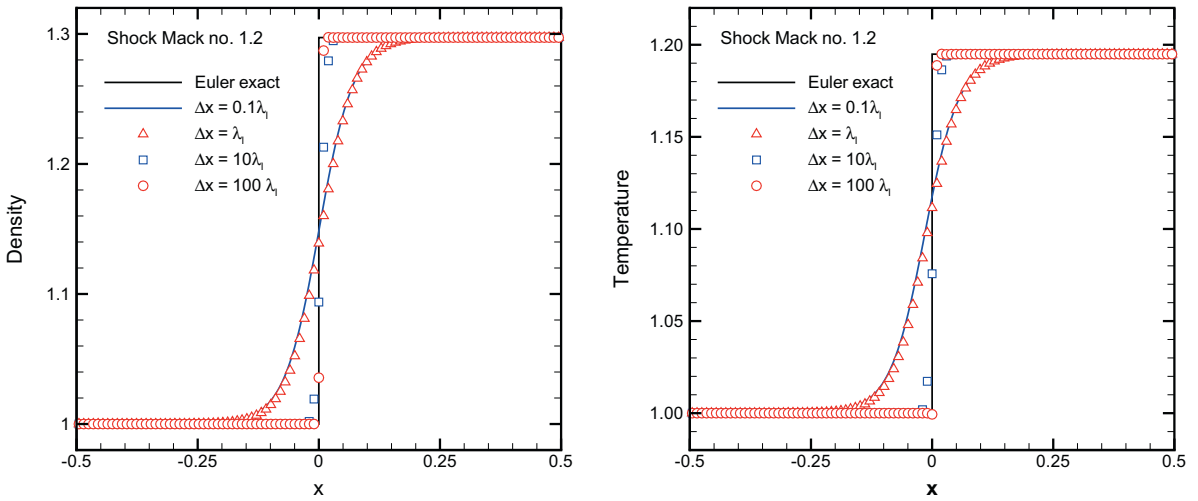

Fig. 9. Unified BGK for $M = 1.2$ shock structure calculations with variable cell sizes and uniform time step determined by CFL = 0.95.

for the shock structure study. It is much easier to evaluate the correctness of the physical and numerical modeling of the scheme, such as the capability to capture the highly non-equilibrium flow behavior.

First we present test cases on the shock structure for argon gas at $M = 1.2$ with $Pr = 2/3$. Ohwada solved the full Boltzmann equation for this case [20]. For the hard sphere molecules, the viscosity coefficient $\mu \sim T^{0.5}$ and $Pr = 2/3$, where the x-coordinate is normalized by $\sqrt{\pi}\lambda_1/2$ and λ_1 is the mean free path of the gas molecules at the upstream condition. Fig. 7 shows the density, temperature, stress and heat flux of an argon shock structure. Comparisons of the results from the unified scheme are made with the solutions of the Boltzmann equation. The results from the direct Boltzmann solver and the current solutions have good agreement. At Mach number 1.2, where the local Knudsen numbers are less than 0.02, as expected, the standard Navier–Stokes equations suffice. The current solution also indicates that the unified scheme can capture accurately the NS solutions.

Next we are trying to get Mach 8 argon shock structure from the unified scheme. Fig. 8 shows the shock structures for viscosity coefficient $\mu \sim T^{0.81}$ at both $Pr = 1.0$ and $Pr = 2/3$. At the same time, the DSMC solution is included for comparison [4]. From this figure, we can clearly observe the effectiveness of the Prandtl number fix in the unified scheme. With the modification of heat flux, the numerical solution gets much better match with the DSMC solution. In comparison with many other DOM solutions for the shock structure [19], the current result from the unified scheme is definitely favorable.

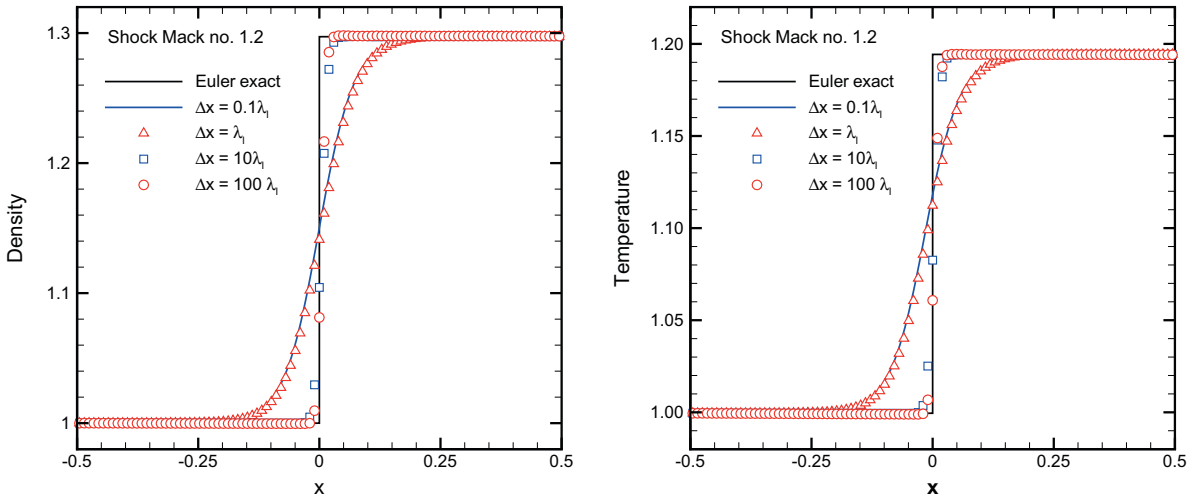

Fig. 10. DOM–Shakhov for $M = 1.2$ shock structure calculations with variables cell sizes. The time step has to be changed from CFL = 0.95 ($\Delta x = 0.1\lambda_1$) to CFL = 0.1 ($\Delta x = 100\lambda_1$). Otherwise, the solutions will blow up.

Case (4). From shock structure resolving to shock capturing scheme

The last test case is related to the shock wave as well. However, instead of fully resolving the shock structure, we are going to change the cell size, from the well resolved case to highly under-resolved one. For the Mach number 1.2 shock structure calculation, the unified scheme uses a time step with a fixed CFL = 0.95. As the increasing of cell size, i.e., $\Delta x = 0.1\lambda_1$, λ_1, $10\lambda_1$, $100\lambda_1$ with the upstream particle mean free path λ_1, the time step used by the unified scheme is increasing. Fig. 9 presents both density and temperature distributions from the unified scheme. Due to the variation of cell size, the scheme changes from a shock structure resolving method to the shock capturing scheme. With $\Delta x = 100\lambda_1$, the unified scheme basically goes to the Euler solution and the shock transition is captured sharply. For the same test case, when a DOM–BGK method is used, the CFL number for the time step has to be changed. With the increasing of mesh size, the CFL number has to be reduced. For example, at $\Delta x = 100\lambda_1$, it is found that the DOM–BGK scheme needs to use a time step with CFL = 0.1. Otherwise, the solution will blow up. Fig. 10 presents the solution from DOM method with kinetic Shahkov model [28]. Even with the same reconstruction scheme, in the under-resolved case, i.e., $\Delta x = 100\lambda_1$, the number of transition points in the shock layer clearly indicates that the numerical dissipation of the DOM–Shahkov method is much larger than that of the unified scheme. The reducing of the numerical dissipation in the unified scheme is mainly due to the inclusion of particle collisions in the flux evaluation across a cell interface.

6. Conclusion

In this paper, we present a unified kinetic approach for flows in the entire Knudsen number. The validity of the approach is based on its full representation of particle movement, i.e., transport and collision. Different from many other approaches, the critical step is that the integral solution of the kinetic model is used in the flux evaluation across the cell interface. The integral solution gives an accurate representation in both continuum and free molecule flows. The current scheme can be considered as a dynamic hybrid method, where the different flow behavior is obtained through the different limits of the integral solution of a single kinetic equation, instead of solving different governing equations in different flow regimes. The weakness for the most existing kinetic methods is that a purely upwinding technique is used in the flux evaluation for the transport term uf_x, which is equivalent to solving the collisionless Boltzmann equation and its solution is only a partial solution of the integral solution used in the unified scheme. Theoretically, the Boltzmann equation is a statistical model with a continuous particle transport and collision process in space and time. So, there is no reason to believe that these particles which transport across the cell interface will not suffer particle collision during its movement toward the cell interface. Therefore, an "exact" integral solution of the full kinetic equation has to be used and it is the key for the success of the unified scheme. Due to its multiscale nature of the unified scheme, through the update of macroscopic flow variables the heat flux of the scheme can be modified according to correct Prandtl number.

The numerical tests presented in this paper validate the current approach in both continuum and rarefied flow regime. For the continuum flow at high Reynolds number, a standard CFL condition for the macroscopic NS equations can be used to determine the time step in the unified scheme, which is much larger than the particle collision time. At the same time, the capability of capturing highly non-equilibrium distribution inside high Mach number shock layer and the free molecule limit has been validated. Overall, the unified scheme is an AP method for the kinetic BGK equation. The method presented in

this paper can be easily extended to 2D and 3D cases. Even though the Prandtl number can be fixed numerically in the multiscale unified scheme, the BGK model is still an approximation of the full Boltzmann equation and the single relaxation is certainly inappropriate. The development of a multiscale unified scheme for the full Boltzmann equation will be an interesting and important research topic.

Acknowledgments

The authors thank Prof. H.Z. Tang for helpful discussion about unified scheme and his help in correcting a few notation mistakes in an early version of this paper. We would also like to thank reviewers for their constructive comments which significantly clarify the idea in the unified scheme. K. Xu was supported by Hong Kong Research Grant Council 621709, National Natural Science Foundation of China (Project No. 10928205), National Key Basic Research Program (2009CB724101), and US National Science Foundation Grant DMS-0914706. J.C. Huang was supported by National Science Council of Taiwan through Grant No. NSC 96–2221-E-019–067-MY2.

References

[1] V.V. Aristov, Direct Methods for Solving the Boltzmann Equation and Study of Nonequilibrium Flows, Kluwer Academic Publishers, 2001.
[2] M. Bennoune, M. Lemou, L. Mieussens, Uniformly stable numerical schemes for the Boltzmann equation preserving the compressible Navier–Stokes asymptotics, J. Comput. Phys. 227 (2008) 3781–3803.
[3] P.L. Bhatnagar, E.P. Gross, M. Krook, A model for collision processes in gases I: small amplitude processes in charged and neutral one-component systems, Phys. Rev. 94 (1954) 511–525.
[4] G.A. Bird, Molecular Gas Dynamics and the Direct Simulation of Gas Flows, Oxford Science Publications, 1994.
[5] J.F. Bourgat, P. Le Tallec, M.D. Tidriri, Coupling Boltzmann and Navier–Stokes equations by friction, J. Comput. Phys. 127 (1996) 227–245.
[6] S. Chapman, T.G. Cowling, The Mathematical Theory of Non-uniform Gases, Cambridge University Press, 1990.
[7] C.K. Chu, Kinetic-theoretic description of the formation of a shock wave, Phys. Fluids 8 (1965) 12.
[8] F. Coron, B. Perthame, Numerical passage from kinetic to fluid equations, SIAM J. Numer. Anal. 28 (1991) 26–42.
[9] P. Degond, J.G. Liu, L. Mieussens, Macroscopic fluid models with localized kinetic upscale effects, Multiscale Model. Simul. 5 (2006) 940–979.
[10] S.M. Deshpande, A Second Order Accurate, Kinetic-Theory Based, Method for Inviscid Compressible Flows, NASA Langley Technical Paper No. 2613, 1986.
[11] F. Filbet, S. Jin, A class of asymptotic preserving schemes for kinetic equations and related problems with stiff sources, J. Comput. Phys. (2010) 7625–7648.
[12] M.N. Kogan, Rarefied Gas Dynamics, Plenum Press, New York, 1969.
[13] V.I. Kolobov, R.R. Arslanbekov, V.V. Aristov, A.A. Frolova, S.A. Zabelok, Unified solver for rarefied and continuum flows with adaptive mesh and algorithm refinement, J. Comput. Phys. 223 (2007) 589–608.
[14] Q.B. Li, S. Fu, On the multidimensional gas-kinetic BGK scheme, J. Comput. Phys. 220 (2006) 532–548.
[15] Q.B. Li, S. Fu, K. Xu, A high-order gas-kinetic Navier–Stokes solver, J. Comput. Phys. (2010) 6715–6731.
[16] Z.H. Li, H.X. Zhang, Gas-kinetic numerical studies of three-dimensional complex flows on spacecraft re-entry, J. Comput. Phys. 228 (2009) 1116–1138.
[17] G. May, B. Srinivasan, A. Jameson, An improved gas-kinetic BGK finite-volume method for three-dimesnional transonic flow, J. Comput. Phys. 220 (2007) 856–878.
[18] L. Mieussens, Discrete-velocity models and numerical schemes for the Boltzmann-BGK equation in plane and axisymmetric geometries, J. Comput. Phys. 162 (2000) 429–466.
[19] L. Mieussens, H. Struchtrup, Numerical comparison of Bhatnagar–Gross–Krook models with proper Prandtl number, Phys. Fluids 16 (2004) 2797–2813.
[20] T. Ohwada, Structure of normal shock waves: direct numerical analysis of the Boltzmann equation for hard-sphere molecules, Phys. Fluids A 5 (1993) 217.
[21] T. Ohwada, On the construction of kinetic schemes, J. Comput. Phys. 177 (2002) 156–175.
[22] T. Ohwada, K. Xu, The kinetic scheme for full Burnett equations, J. Comput. Phys. 201 (2004) 315–332.
[23] T. Ohwada, S. Kobayashi, Management of discontinuous reconstruction in kinetic schemes, J. Comput. Phys. 197 (2004) 116–138.
[24] S. Pieraccini, G. Puppo, Implicit–Explicit schemes for BGK kinetic equations, J. Sci. Comput. 32 (2007) 1–28.
[25] D.I. Pullin, Direct simulation methods for compressible inviscid ideal gas flow, J. Comput. Phys. 34 (1980) 231–244.
[26] T.E. Schwartzentruber, I.D. Boyd, A hybrid particle-continuum method applied to shock waves, J. Comput. Phys. 215 (2006) 402–416.
[27] T.E. Schwartzentruber, L.C. Scalabrin, I.D. Boyd, A molecular particle-continuum method for hypersonic non-equilibrium gas flows, J. Comput. Phys. 225 (2007) 1159–1174.
[28] E.M. Shakhov, Generalization of the Krook kinetic equation, Fluid Dyn. 3 (1968) 95.
[29] M.D. Su, K. Xu, M. Ghidaoui, Low speed flow simulation by the gas-kinetic scheme, J. Comput. Phys. 150 (1999) 17–39.
[30] S. Tiwari, Coupling of the Boltzmann and Euler equations with automatic domain decomposition, J. Comput. Phys. 144 (1998) 710–726.
[31] E. Toro, Riemann Solvers and Numerical Methods for Fluid Dynamics, Springer, 1999.
[32] H.S. Wijesinghe, R.D. Hornung, A.L. Garcia, N.G. Hadjiconstantinou, Three-dimensional hybrid continuum-atomistic simulations for multiscale hydrodynamics, J. Fluid Eng. 126 (2004) 768–777.
[33] K. Xu, Numerical hydrodynamics from gas-kinetic theory, Ph.D. Thesis, Columbia University, 1993.
[34] K. Xu, A gas-kinetic BGK scheme for the Navier–Stokes equations and its connection with artificial dissipation and Godunov method, J. Comput. Phys. 171 (2001) 289–335.
[35] K. Xu, Z.W. Li, Dissipative mechanism in Godunov-type schemes, Int. J. Numer. Methods Fluids 37 (2001) 1–22.
[36] K. Xu, M.L. Mao, L. Tang, A multidimensional gas-kinetic BGK scheme for hypersonic viscous flow, J. Comput. Phys. 203 (2005) 405–421.
[37] K. Xu, X. He, C. Cai, Multiple temperature kinetic model and gas-kinetic method for hypersonic nonequilibrium flow computations, J. Comput. Phys. 227 (2008) 6779–6794.
[38] J.Y. Yang, J.C. Huang, Rarefied flow computations using nonlinear model Boltzmann equations, J. Comput. Phys. 120 (1995) 323–339.